A sustainable and profitable biorefinery strategy: Efficiently converting lignocellulose to furfural, glucose and phenolic compounds

Chao Liu[a, b], Tingting Cai[a], Xiaoyan Yin[a], Jie Liang[a], Shuya Jia[c], Xiaolei Zhang[c], Junming Xu[a, b], Jun Hu[d], Jianchun Jiang[a, b *], Kui Wang[a, b *]

[a]*Institute of Chemical Industry of Forest Products, Chinese Academy of Forestry; Key Lab. of Biomass Energy and Material, Jiangsu Province; National Engineering Lab. for Biomass Chemical Utilization, Nanjing 210042, China*

[b]*Co-Innovation Center of Efficient Processing and Utilization of Forest Resources, Nanjing Forestry University, Nanjing 210037, China*

[c]*Department of Chemical and Process Engineering, University of Strathclyde, Glasgow G1 1XJ, UK*

[d]*School of Chemical Engineering, Northwest University, Xi'an 710069, China*

[*]*Corresponding author emails: jiangjc@icifp.cn , wangkui@caf.ac.cn*

Abstract

Sustainability and profitability of a biorefinery is based on the efficient utilized of all components of lignocellulosic biomass. However, the resistance of lignocellulosic structure and the differences in physicochemical properties of its main components are typical challenges for most lignocellulosic fractionation approaches. Here, we demonstrate a fractionation strategy that is able to efficiently fractionate the whole lignocellulose component and convert it into a range of valuable products. The core of our method is to maintain the quality of lignin components by adding isopropanol while formic acid and molten salt hydrate ($LiCl{\cdot}3H_2O$) promote the dissolution of hemicellulose and lignin. Subsequently, as-obtained cellulose is readily saccharified due to invasion of dense crystal structure, and enzymatic hydrolysis yields 728.3 mg/g glucose. After simple separation, a 75.6 mol% of furfural was produced from hemicellulose in $LiCl{\cdot}H_2O$/γ-valerolactone (GVL) biphasic system, and 75.7 wt% phenolic mono-/oligomer were produced from lignin hydrolyzed in formic acid/isopropanol$_{(aq)}$. Attributed to this rational design, the techno-economic analysis predicts a revenue of 122.66 USD by processing 100 kg of waste bamboo using the

This is a peer-reviewed, accepted author manuscript of the following article: Liu, C., Cai, T., Yin, X., Liang, J., Jia, S., Zhang, X., Xu, J., Hu, J., Jiang, J., & Wang, K. (2022). A sustainable and profitable biorefinery strategy for efficiently converting lignocellulose to furfural, glucose and phenolic compounds. Green Chemistry, 24(21), 8494-8502. https://doi.org/10.1039/d2gc03231g

above developed approach. In this process, all solvents participate in both fractionation and catalytic conversion and are allowed to be recycled, which is in line with the principles of green chemistry.

Keywords: lignocellulosic biomass, biorefinery, molten salt hydrate, solvent effects, furfural

Introduction

The reduction of fossil energy reserves and climate problems caused by greenhouse gas emissions force people to develop and use renewable energy.[1-3] As a kind of renewable energy with abundant reserves and wide distribution, lignocellulose is one of the important raw materials to replace fossil energy. lignocellulose is mainly composed of cellulose (35-50%), hemicellulose (25-30%) and lignin (15-30%), the relative amount of each structural component depends on the species.[4, 5] Biorefinery represents a process that converts lignocellulosic biomass to energy and other beneficial byproducts (*i.e.*, biochemicals, biomased materials). However, the inherent structural complexity of lignocellulosic and the significant differences in physicochemical of its components have become important challenges in the biorefinery process.[6-8]

In traditional biorefinery, lignocellulose is usually delignified initially with high intensity pretreatment to obtain high-quality carbohydrates for use in the pulp and paper industry or bioethanol production (**Figure. 1a**).[9-11] In this process, the high pretreatment severities not only leads to a large loss of hemicellulose, but also the removed lignin contains a large number of

relatively inert C-C interunit linkages. The significant changes in the chemical structure of lignin make it a low value resource for the production of aromatic compounds, which are commonly burned to generate heat.[12-14] To address this problem, the "reductive catalytic fractionation (RCF)" strategy based on the "lignin-first" biorefinery was proposed by group of Sels and Abu-Omar in 2015 (**Figure. 1b**).[15, 16] In this strategy, lignin is dissolved and depolymerized in alcohol solvent to obtain lignin oil (*i.e.*, phenolic monomers, dimers and oligomers) under reductive atmosphere with the heterogeneous metal catalyst, while carbohydrates are retained in the solid residue for further processing. This strategy represents significant progress in an integrated lignocellulose biorefinery, and unlocked the novel approaches for the fractionation of lignin conversion to high yield phenolic compounds.[17-19] However, several critical challenges remained in the "lignin-first" biorefinery. Firstly, although the lignin-oil obtained from lignin has high yield of phenolic monomer (up to 60%, chemical science),[20] applications are still restricted by the complicated isolated components. Besides, a lot of hemicellulose was modified or lost in "lignin-first" strategy, preventing their further conversion to valuable products. These considerations, combined with low efficient recovery of expensive catalysts, rendered a reduced efficiency and techno-economic balance for a cost-effective integrated lignocellulose biorefinery.

The aim of this work was explored the prospect of sustainable and profitable fractionation strategy and full-component conversion of lignocellulose, while considering and whenever possible,

implementing the main principles of green chemistry (**Figure. 1c**).[21, 22] The proposed integrated biorefinery that simultaneously produces furfural, useful mono-/oligo phenolics, as well as a readily enzymatic hydrolysable cellulose to achieve a high carbon and mass efficiency (**Figure. 1d**). In our opinion, this biorefinery protocol will provide a clear incentive for the production of profitable, sustainable chemicals with a low carbon footprint through the overall bio-refining of renewable lignocellulose.

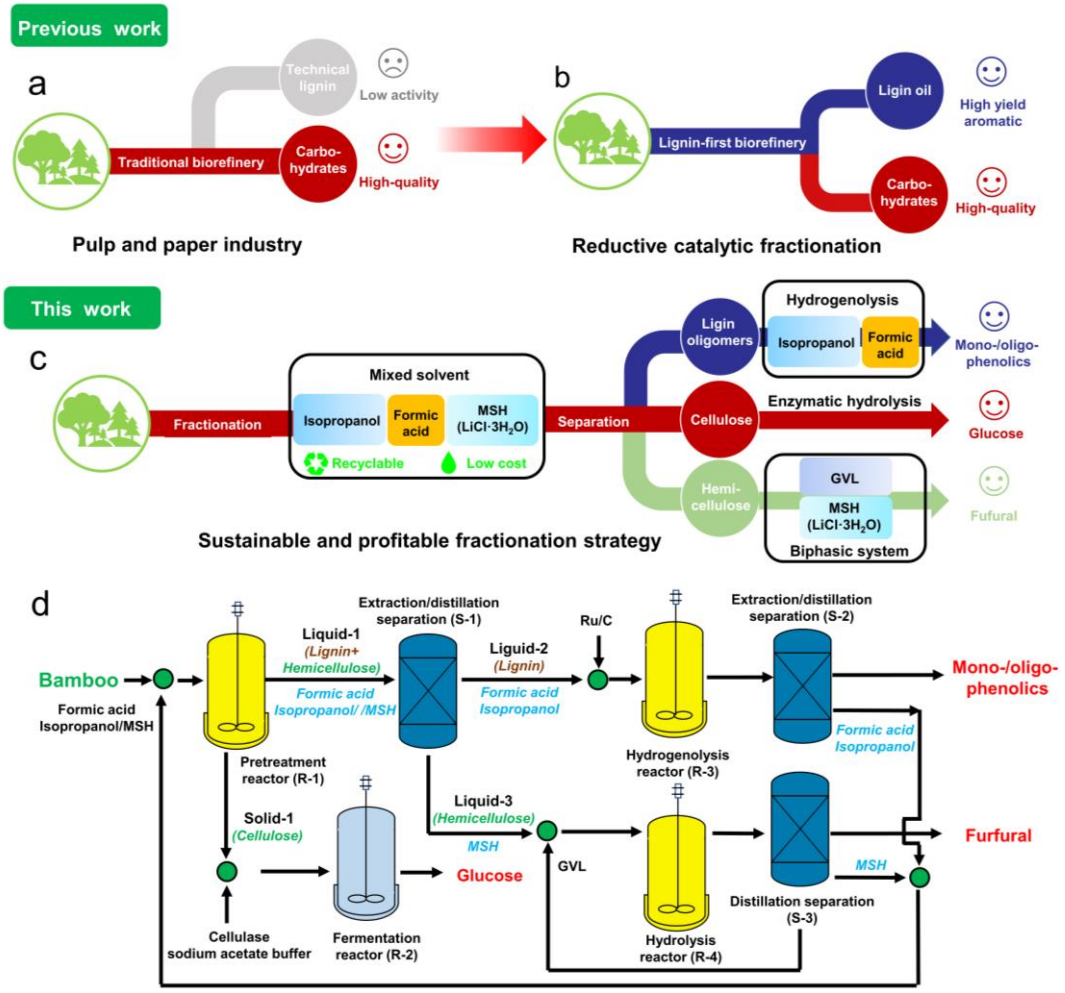

Figure 1. Overview of biorefinery strategy. **a**: Traditional biorefinery approaches is heavily carbohydrates-centered, and for use in the pulp and paper industry. **b**: Reductive catalytic fractionation, focused on high yield lignin derived aromatic and carbohydrates. **c**. This work: lignocellulose fractionation and full-component conversion. **d**. Proposed comprehensive biorefinery process for furfural, glucose and phenolic compounds.

Results and discussion

Overview of the pretreatment

The first step of our process, a recyclable mixed solvent system consisting of isopropanol and molten salt hydrate (MSH, $LiCl{\cdot}3H_2O$) was used for hemicellulose and lignin dissolution from lignocellulose under the formic acid catalyst. Several different pretreatment operating parameters such as temperature, time, formic acid load and MSH/isopropanol solvent ratio were evaluated during the first fractionation (**Figure 2a-d**). The best fractionation efficiency of 86.26% cellulose retention (**Figure 1d, Solid-1**) was obtained at 140 ℃ for 1.5 h in the MSH/isopropanol (30g/20g) mixed solvent under 1.5 g formic acid. After that, 93.19% of lignin and 91.81% of hemicellulose were dissolved in **Liquid-1**, and then facile separated by a simple extractive distillation operation. On the one hand, the addition of formic acid is beneficial to the dissolution/depolymerization of carbohydrates and lignin. On the other hand, acid-catalyzed lignin dissolution/depolymerization generally results in a low yield of phenolic monomers during subsequent hydrolysis due to the large amount of recondensation that occurs to form stubborn C-C bonds under these conditions (**Figure 2e**).[23-25] The biorefining strategy established in this study could derivatization/protected lignin based on the fact that alcohols or diols can capture carbocation species formed by lignin intermediates under acidic conditions (**Figure 2f**).[26, 27]

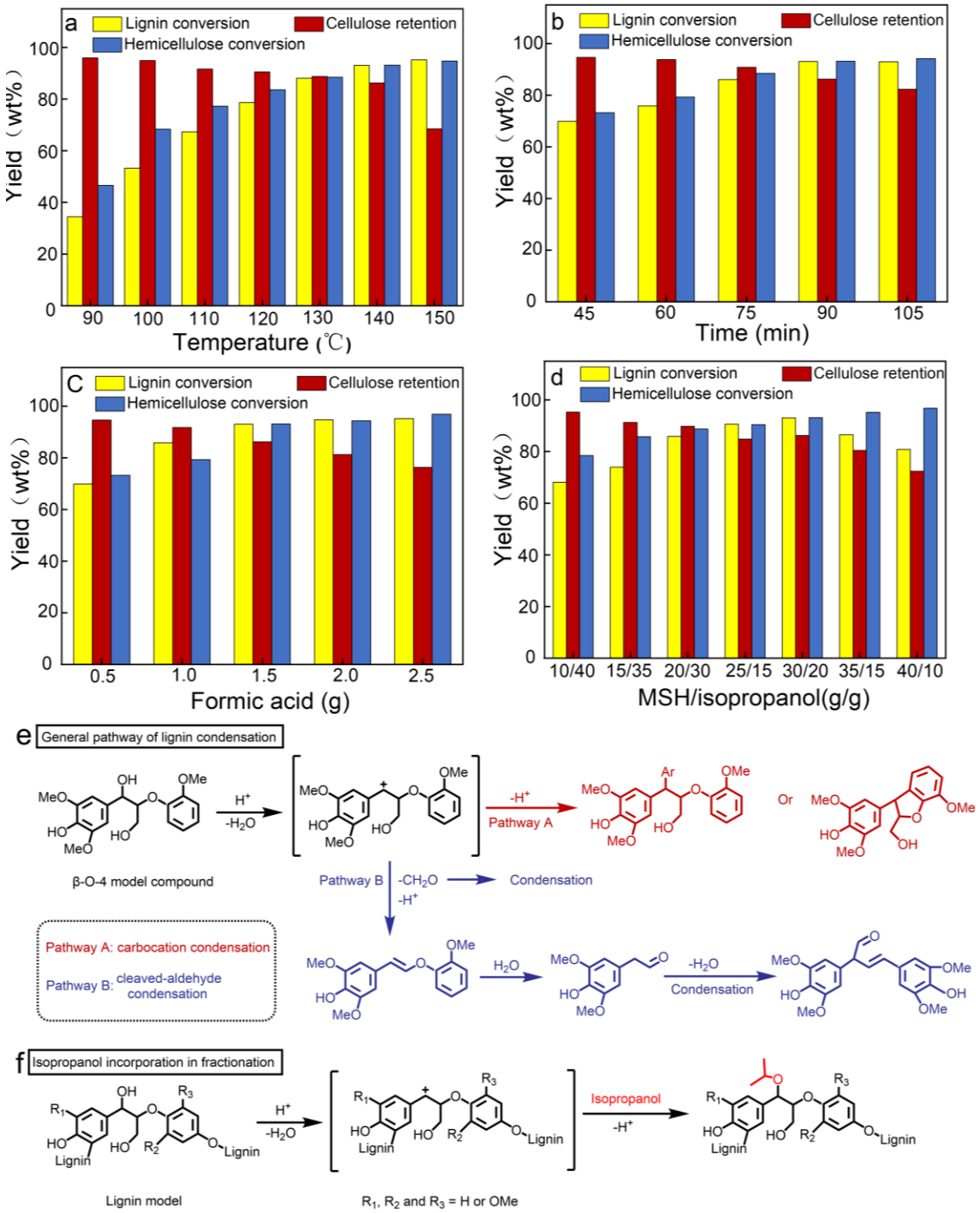

Figure 2. Pretreatment parameters screen for the fractionation of raw bamboo biomass. **a**: Pretreatment temperature (2.5 g bamboo, 1.5 g formic acid, MSH/isopropanol=30/20 g, 1.5 h and 2 Mpa N_2). **b**: Pretreatment time (2.5 g bamboo, 1.5 g formic acid, MSH/isopropanol=30/20 g, 140 ℃ and 2 Mpa N_2). **c**. Formic acid load (2.5 g bamboo, MSH/isopropanol=30/20 g, 2 Mpa N_2, 140 ℃ for 1.5 h). **d**: Solvent ratio (2.5 g bamboo, 1.5 g formic acid, 2 Mpa N_2, 140 ℃ for 1.5 h). **e**: Recondensation pathways in lignin acidolysis. **f**: Derivatization/protection pathways in lignin acidolysis.

Cellulose enzymatic hydrolysis and lignin extraction

The cellulose-rich **Solid-1** (Cellulose purity: 90.4 wt%) from the native plant cell wall and its subsequent enzymatic hydrolysis conversion to glucose are illustrated in **Figure. 3a**. Enzymatic hydrolysis of **Solid-1** was implemented to evaluate the potential improvements or impacts of first-step pretreatment on glucose release. Raw bamboo biomass, microcrystalline cellulose (MCC) and **Solid-1** were enzymatically hydrolysed using general commercially cellulase. Unsurprisingly, the raw bamboo biomass showed low cellulase hydrolysis efficiency, only 43.22 mg/g of glucose yield could be obtained after 72h incubation (**Figure. 3b**). This result is due to the poor accessibility of cellulose due to the dense secondary wall and complex spatial structure of the bamboo.[28, 29] In contrast, the enzymatic hydrolysis efficiency of MCC was significantly improved due to its simple spatial structure, and 526.10 mg/g of glucose yield could be obtained. Furthermore, the **Solid-1** achieves the highest glucose yield of 728.30 mg/g under the same conditions, which is 16.5 times that of the bamboo. The significant improvement of enzymatic hydrolysis efficiency can be attributed to the following two points: 1) In the process of pretreatment, the non-cellulose fraction are largely removed and cellulose purity was up to 90.4%; 2) Compared with the MCC, the lower crystallinity, higher free hydroxyl content, fewer hydrogen bonds and particle size of cellulose in **Solid-1**, which was proved by XRD, FTIR peak-differentiating and imitating, laser particle size analysis. (**Figure. 3c-e**). This effect was attributed to formic acid and MSH ($LiCl{\cdot}3H_2O$) promote the dissolution of lignin and hemicellulose in the bamboo and also affect cellulose, which is decoupled by partial destruction of the crystallization region, hydrogen bond network and exposure of free hydroxyl groups.

Next, we moved to the separation operation of **Liquid-1** consisting of hemicellulose and lignin fraction, and the process flow chart are illustrated in **Figure. 3f**. First, from the **Liquid-1**, solvent system (Formic acid and isopropanol aq) was readily isolated by vacuum distillation. Moreover, the hemicellulose derivatives are dissolved

in water to form **Liquid-3**, while the lignin fragments from the solid residues are extracted with CH_2Cl_2. Finally, after the CH_2Cl_2 is removed by vacuum distillation, the lignin fragment is remixed with the solvent system to form **Liquid-2**.

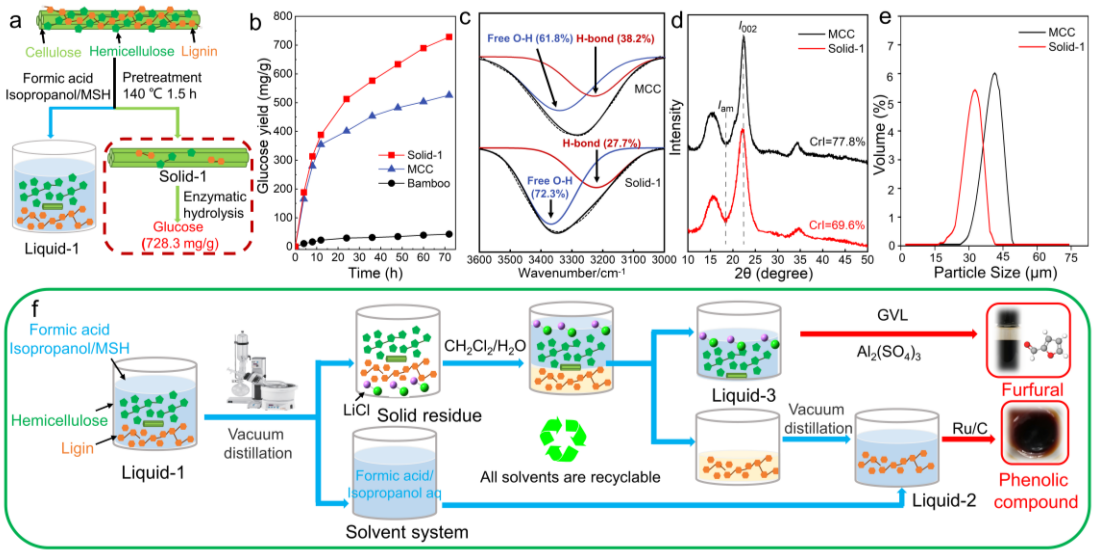

Figure. 3 a: Schematic illustration of cellulose fractionation and conversion. **b:** The glucose yield of the raw bamboo biomass, MCC and solid-1 enzymatic hydrolysis. **c:** FTIR spectra peak-differentiating and imitating. **d:** XRD. **e:** Volume-based particle size distribution**. f:** Flow chart of separation process of lignin and hemicellulose fraction.

Lignin depolymerization

After the above extraction-distillation operation, **Liquid-2** mainly consisting of lignin fragment and hydrogen-donor solvent, which was hydrogenized assisted via various catalysts (e.g., Pd/C, Pt/C, Rh/C, and Ru/C) (**Figure. 4a and b**). GC-MS analysis showed that Ru/C showed the best catalytic performance, which was obtained 25.6 wt% phenolic monomer yield and 50.1 wt% phenolic oligomer based on lignin in **Liquid-2**. The reason may be that among the above-mentioned commercial catalysts, Ru/C has the highest catalytic activity for cleaving C-O bonds.[30, 31] More details of the results obtained by over different catalysts were shown in Table S1**,** and phnolic monomer obtained by hydrotreating by Ru/C catalyst were identified by GC-MS shown in **Figure. 4f**.

GPC analysis showed that the Mw/Mn of lignin (in **Liquid-2**) decreased from 1159/814 Da (Mw > 700 Da accounting for 54.5%) to 853/716 Da (Mw > 700 Da accounting for 15.2%) (**Figure. 4a**). These results suggested that lignin was efficiently converted into a yield of 75.7wt% phenolic monomers/oligomers catalyzed by Ru/C.

To reveal the details of the lignin depolymerization process, the **Liquid-2** and the products obtained at 220 ℃ for 4 h were analyzed by ESI-MS (**Figure. 4c and d**). After hydrotreating, the characteristic peak response value of m/z=400~700 decreases sharply or disappears, while the characteristic peak of m/z =100~400 increases significantly. These results indicate that a large number of polymers are depolymerized into monomers or oligomers of lignin with lower molecular weight during **Liquid-2** hydrolysis. Moreover, the possible structures of several easily (green) and refractory (gray) polymeric polymers are speculated, as shown in **Figure 4e**. Easily depolymerized polymers can usually depolymerize to form typical phenolic monomers such as guaiacol and 4-methy phenol by breaking low bond energy β-O-4 bonds (290~305 kJ/mol).[32-34] The refractory structures also had the common structural features of benzene rings connected directly by C-C bonds, or one benzene ring connected to the alpha carbon of another, and their bond energies are typically 360-490 kJ/mol.[35-37] Therefore, compared with the easily depolymerized polymer, the presence of high bond energy C-C bonds in the refractory polymer makes it difficult to hydrolyze. Furthermore, to investigate the structural changes of the side-chains and aromatic regions of **Liquid-2** before and after depolymerization, 2D HSQC NMR was used. Figure. 4f-g and Figure. S2 show the side-chain (δC/δH=50-95/2.5-6.0) and aromatic regions (δC/δH=100-150/5.5-8.5) of the Liquid-2 and depolymerized product spectra,

respectively. The assignment information of the cross signals in the spectrogram is derived from the previously literature[38, 39] and is detailed in Table. S2. In the side-chains region, the lignin structure of the depolymerized products changed significantly compared with that of **Liquid-2**. In addition to the signal of the Ar-OCH_3, other previously existing crossover signals are replaced by new signals P γ-OCH_3, P γ-OH and β-β. Based on the previously reported[40] signals of lignin condensation structure, the weak cross signals in the Condensed-I and Condensed-II regions may be attributed to the refractory structure of Liquid-2 or the newly formed condensation structure. In the aromatic region, except for G_2, G_5 and G_6 cross-signals still exist in the depolymerized product, other cross-signals are replaced by some unknown signals. In summary, the observations indicate that the structure of **Liquid-2** changes significantly during the hydrogenolysis process, and monomers and oligomers are obtained, accompanied by some condensation products and substances with unidentified structures.

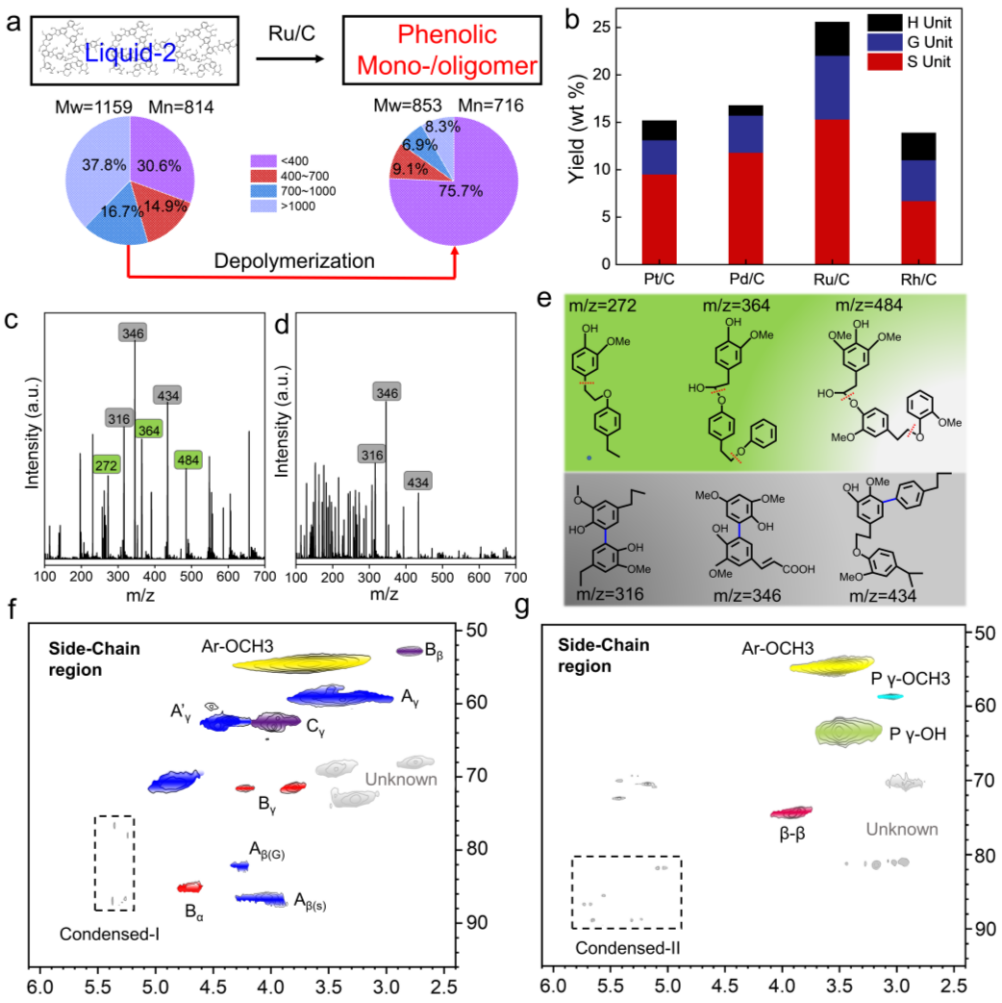

Figure. 4 a: Schematic illustration of lignin fragment depolymerization to aromatic. **b:** The yield of phenolic monomers obtained over different catalysts. **c:** ESI-MS spectra of liquid-2 and **d:** reaction at 220 ℃ for 4 h. **e:** Possible oligomer structure in Liquid-2 with easy (green) and refractory (gray) depolymerization. 2D HSQC NMR spectrum of **f:** liquid-2 and **g**: reaction at 220 ℃ for 4 h.

Hemicellulose conversion to furfural

The **Liquid-3** mainly consisting of hemicellulose derivatives and MSH ($LiCl{\cdot}3H_2O$), subsequent conversion to furfural catalyzed by $Al_2(SO_4)$ in GVL solvent was illustrated in **Figure. 5a**. The addition of GVL can form a biphasic system with MSH and promote xylan conversion, which has been reported in our previous literature.[41] In order to reveal the mechanism of GVL promoting furfural production, the interaction energy functions of furfural, water and GVL were calculated (**Figure. 5b and c**). It should be noted that a lower intermolecular interaction energy indicates a stronger attraction between molecules. Therefore, furfural molecules

are extracted from water to GVL layer due to $E_{mix\text{-}GVL}$=0.48 < $E_{mix\text{-}H2O}$=2.78, and the higher temperature further promoted the attraction between GVL and furfural (**Figure. 5c**). Besides, the strong interaction between GVL and furfural molecules can provide a protective shell for furfural molecules and prevent the polymerization of furfural into humins, which is consistent with previous reports. High-performance anion exchange chromatography (HPACE) and liquid chromatography (HPLC) were used to determine the components in **Liquid-3**.[42] The results showed that the main components of **Liquid-3** are oligosaccharides (49.71 wt%, derived from hemicellulose), xylose (34.18 wt%), glucose (8.25 wt%) furfural (4.49 wt%), and others (3.37 wt%, e.g., acetic acid, arabinose and galactose) (**Figure. 5e**). These results illustrate the fact that hemicellulose depolymerizes to oligosaccharides, xylose and other small molecular products during fractionation, which is conducive to its further catalytic conversion to furfural.[43, 44] A 75.6 mol% of furfural conversion in the biphasic solvent was achieved under optimized conditions (140 °C for 60 min), which is comparable to the maximum xylan-to-furfural conversion yield, but significantly less process time. Energy consumption analysis suggests that to produce a considerable amount of furfural, the energy consumed by commercial xylan is 1.73 times (1.656 kWh) that of as-obtained hemcellulose (0.956 kWh), which confirms the above statement that **Liquid-3** is more convertible.

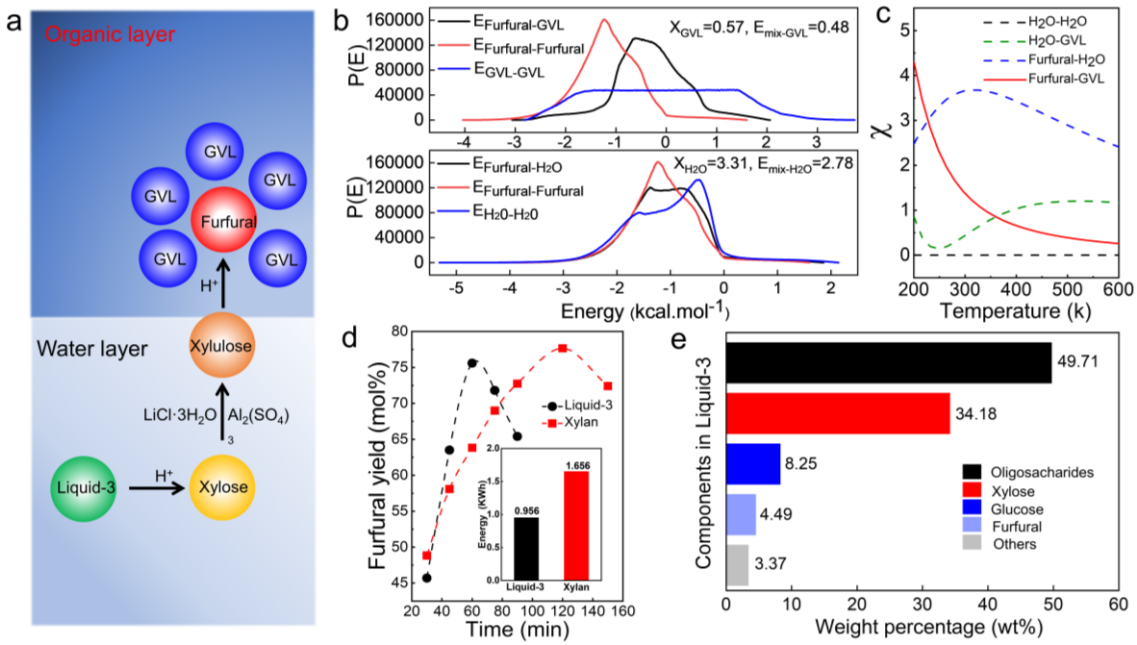

Figure. 5 a: Schematic illustration of Liquid-3 conversion to furfural. **b:** The interaction distribution function curve between different molecules. **c:** The interaction energy curve with temperature and **d:** Conversion yield of Liquid-3/GVL and Xylan in $LiCl{\cdot}3H_2O$/GVL to furfural at 140 °C catalyzed by $Al_2(SO_4)$; The energy consumption of Liquid-3 or xylan to produce equivalent furfural, reactor power: 1000W. **e:** Components in Liquid-3.

Comprehensive mass balance of biorefinery strategy

Based on the obtained experimental data, a process model was developed to perform a technical-economic analysis (TEA) of the bamboo fractionation and conversion process. The TEA of our designed biorefinery was calculated for convert 100 kg of waste bamboo. After the pretreatment, bamboo was divided into solid and liquid parts, the cellulose rich **Solid-1** and the lignin rich, hemicellulose rich **Liquid-1**. Based on the preprocessing efficiency in the previous section (Figure 2a-d), the main components in **Solid-1** and **Liqui-1** are quantitatively shown in Figure 6a. Subsequently, **Solid-1** was used to enzymatic hydrolysis to obtain glucose, accompanied by a certain amount of C5 and C6 sugars derived. Moreover, the extraction separation operation divides **Liquid-1** into **Liquid-2** containing 23.32 kg lignin and **Liquid-3** containing 26.36

kg hemicellulose and 6.00 kg cellulose. Finally, **Liquid-2** was hydrogenolysis to produce lignin monomers and oligomers, and **Liquid-3** was hydrolysis to produce furfural in a biphasic system. It should be noted that the production of furfural is accompanied by the formation of soluble and insoluble polymers. Obviously, the insoluble polymer can be easily removed by filtration operation. The soluble polymer can be removed by activated carbon adsorption, and the activated carbon after adsorption can be regenerated at high temperature.[45] Consequently, in this process, 27.20 kg glucose, 14.40 kg furfural, 25.40 kg phenolic compounds, 18.72 kg sugars derived (for bioethanol) and 11.60 kg H_2O could be obtained from the waste bamboo. The assumptions made in this process, raw materials and product pricing are available in Table S3. Market investigation showed that the price of glucose and furfural is 136.00 USD and 216.00 USD, respectively. The depolymerizing product of lignin is considered lignin oil and its pricing is based on the lowest forecast price reported in the literature.[18] Labor cost (188.16 USD) is the biggest contributor to the costs, which comes from the equipment operation part (134.40 USD) and the products separation part (53.66 USD). It is worth noting that the power cost of separation operation is 20.30 USD, higher than the power cost of equipment operation 12.84 USD. Summing the labor and power costs to obtained the separation step costs 74.06 USD, which accounts for about 1/4 of the total cost. Due to the loss of formic acid recovery process, the consumption cost of formic acid is 15.6 USD. Equipment depreciation cost and product storage cost are 13.0 USD and 20.0 USD respectively, which are included in the total cost. The catalyst showed satisfactory recycling performance (Figure. S1), so it was not included in the cost. Overall, the analysis suggests that

our proposed process can generate revenue of 122.66 USD by processing 100 kg of waste bamboo. Therefore, the proposed biorefinery strategy could become an economically competitive alternative to current carbohydrate-centered or lignin- centered fractionation approach.

In order to study the ecological and environmental impacts of the proposed biorefinery strategy, a life cycle assessment (LCA) was conducted. The life cycle model system boundary of bamboo biorefinery is shown in Figure 6c. As this study is based on the waste bamboo biorefinery, the life cycle model does not take bamboo planting process into account in the model. The whole life cycle includes five stages: pretreatment, fermentation, hydrolysis, hydrogenolysis and product separation. It should be noted that all the fractionation steps of bamboo are classified as pretreatment. Details of the various parameters of life cycle assessment can be seen in Table S4-7. As shown in Figure 6d, the pretreatment steps contributed significantly to many environmental factors, including, 93.5% HTP, 67.3% AP and 40.0% ADP. This is attributed to the presence of formic acid emission and power consumption in the pretreatment process, which leads to the increase of HTP, AP and ADP. By the way, Electricity resources are assumed to be derived entirely from fossil fuels such as coal in this life cycle model. The product separation step consumes the most power resources resulting in Greenhouse gas emissions, so it contributes the largest portion of GWP (44.0%). The proportion of the final weighting environmental impact potential for bamboo biorefinery process in comprehensive indicators is shown in Figure 6e. In the proposed biorefinery process, ADP (62.0%) accounts for the largest proportion of environmental impact, followed by AP (30.4%). And meanwhile, the impact of HTP is negligible. Loss of formic acid

recycling and electricity consumption are the main causes of environmental impacts. The proposed biorefinery process can be further improved in future research by reducing energy consumption and improving recovery efficiency.

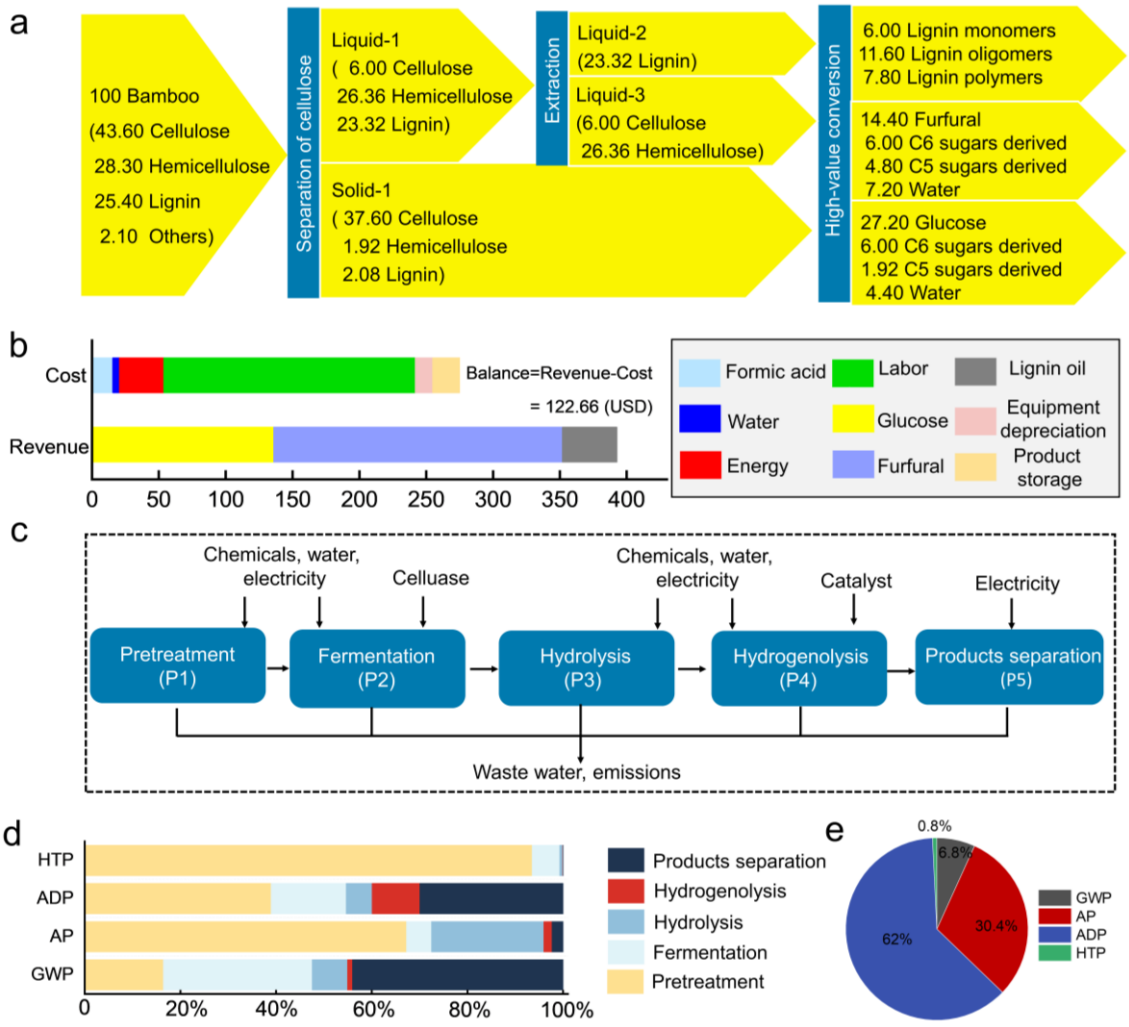

Figure. 6 a: Mass balance for the proposed biorefinery strategy based on bamboo. **b:** Costs and revenues. **c**: LCA system boundary diagram. **d**: Contribution distribution of environmental impact in each process of bamboo biorefinery. **e:** The proportion of environmental impact potential of each link of bamboo biorefinery in the comprehensive index. HTP: Human Toxicity Potential. ADP: Abiotic Depletion Potential. AP: Acidification Potential. GWP: Global Warming Potential. Reaction conditions: separation of cellulose (140 ℃ for 1.5 h, 2Mpa N_2), cellulose enzymatic hydrolysis (50 ℃ for 72 h), hemicellulose hydrolysis (140 ℃ for 1. 0 h, 2 Mpa N_2), lignin hydrogenolysis (220 ℃ for 4 h, 2Mpa H_2).

Conclusion

In summary, we have developed a sustainable and profitable biorefinery strategy in the present study. The

approach can produce valuable glucose from cellulose and furfural from hemicellulose in parallel with high-quality phenolic compouds amenable to further treatment. The rational design enabled a revenue of 122.66 USD by treatment 100 kg of waste bamboo. Moreover, bamboo biomass showed high fractionation efficiency in formic acid-isopropanol/MSH ($LiCl \cdot 3H_2O$) solvent system, and all solvents and catalysts commercially available in this process can be recovered by a simple separation operation. The proposed biorefinery strategy developed in this study may hold the potential for future industrial applications in biorefining due to its system sustainability and economic competitiveness.

Author contributions

Chao Liu: the experiment of fractionation and depolymerization of bamboo was carried out, data collation and analysis, writing manuscript. Kui Wang: conceptualization, methodology, formal analysis. Tingting Cai and Xiaoyan Yin: chemical composition analysis of bamboo and fractionation samples. Jie Liang: product analysis, sample characterization. Shuya Jia: discussion of results of computational simulations. Xiaolei Zhang and Jun Hu: computational simulation, result analysis and review. Junming Xu: writing-review. Jianchun Jiang: funding acquisition, supervision, writing – review.

Competing interests

The authors declare no competing interests.

Acknowledgements

The authors would like to thank Fundamental Research Funds of CAF (No.CAFYBB2022QB001), National Nature Science Foundation of China (31870714), and the Youth Talent Support Program for Science & Technology Innovation of National Forestry and Grassland (2019132603) for

financial support. The work was carried out at Shanxi Supercomputing Center of China, and the calculations were performed on TianHe-2.

Data availability: The authors declare that all of the data that support the findings of this study are available within the article and its Supplementary Information files or from the corresponding author upon reasonable request.

References

1. X. Meng, Y. Pu, M. Li and A. J. Ragauskas, *Green Chem.*, 2020, **22**, 2862-2872.
2. Y. Luo, Z. Zhao, B. Jiang, M. Wei, Z. Zhang, L. Zeng, J. H. Clark and J. Fan, *Green Chem.*, 2022, **24**, 1515-1526.
3. Y. Wan and J.-M. Lee, *ACS Catal.*, 2021, **11**, 2524-2560.
4. Z. Jiang, J. Remón, T. Li, V. L. Budarin, J. Fan, C. Hu and J. H. Clark, *Cellulose*, 2019, **26**, 8383-8400.
5. L. Shuai and J. Luterbacher, *ChemSusChem*, 2016, **9**, 133-155.
6. Z. Sun, G. Bottari, A. Afanasenko, M. C. A. Stuart, P. J. Deuss, B. Fridrich and K. Barta, *Nat. Catal.*, 2018, **1**, 82-92.
7. Y. Liao, S.-F. Koelewijn, G. V. d. Bossche, J. V. Aelst, S. V. d. Bosch, T. Renders, K. Navare, T. Nicolaï, K. V. Aelst, M. Maesen, H. Matsushima, J. M. Thevelein, K. V. Acker, B. Lagrain, D. Verboekend and B. F. Sels, *Science*, 2020, **367**, 1385-1390.
8. S. Van den Bosch, T. Renders, S. Kennis, S. F. Koelewijn, G. Van den Bossche, T. Vangeel, A. Deneyer, D. Depuydt, C. M. Courtin, J. M. Thevelein, W. Schutyser and B. F. Sels, *Green Chem.*, 2017, **19**, 3313-3326.
9. H. Luo, E. P. Weeda, M. Alherech, C. W. Anson, S. D. Karlen, Y. Cui, C. E. Foster and S. S. Stahl, *J Am Chem Soc*, 2021, **143**, 15462-15470.
10. X. Liu, F. P. Bouxin, J. Fan, V. L. Budarin, C. Hu and J. H. Clark, *ChemSusChem*, 2020, **13**, 4296-4317.
11. X. Luo, Y. Li, N. K. Gupta, B. Sels, J. Ralph and L. Shuai, *Angew. Chem. Int. Ed.*, 2020, **59**, 11704-11716.
12. W. Schutyser, T. Renders, S. Van den Bosch, S. F. Koelewijn, G. T. Beckham and B. F. Sels, *Chem. Soc. Rev.*, 2018, **47**, 852-908.
13. C. Li, X. Zhao, A. Wang, G. W. Huber and T. Zhang, *Chem. Rev.*, 2015, **115**, 11559-11624.
14. H. Luo and M. M. Abu-Omar, *Green Chem.*, 2018, **20**, 745-753.
15. S. Van den Bosch, W. Schutyser, R. Vanholme, T. Driessen, S. F. Koelewijn, T. Renders, B. De Meester, W. J. J. Huijgen, W. Dehaen, C. M. Courtin, B. Lagrain, W. Boerjan and B. F. Sels, *Energy Environ. Sci.*, 2015, **8**, 1748-1763.
16. T. Parsell, S. Yohe, J. Degenstein, T. Jarrell, I. Klein, E. Gencer, B. Hewetson, M. Hurt, J. I. Kim, H. Choudhari, B. Saha, R. Meilan, N. Mosier, F. Ribeiro, W. N. Delgass, C. Chapple, H. I. Kenttämaa, R. Agrawal and M. M. Abu-Omar, *Green Chem.*, 2015, **17**, 1492-1499.
17. K. Van Aelst, E. Van Sinay, T. Vangeel, E. Cooreman, G. Van den Bossche, T. Renders, J. Van Aelst, S. Van den Bosch and B. F. Sels, *Chem. Sci.*, 2020, **11**,

11498-11508.

18. A. W. Bartling, M. L. Stone, R. J. Hanes, A. Bhatt, Y. Zhang, M. J. Biddy, R. Davis, J. S. Kruger, N. E. Thornburg, J. S. Luterbacher, R. Rinaldi, J. S. M. Samec, B. F. Sels, Y. Román-Leshkov and G. T. Beckham, *Energy Environ. Sci.*, 2021, **14**, 4147-4168.
19. T. Ren, S. You, Z. Zhang, Y. Wang, W. Qi, R. Su and Z. He, *Green Chem.*, 2021, **23**, 1648-1657.
20. Z. Sun, B. Fridrich, A. de Santi, S. Elangovan and K. Barta, *Chem. Rev.*, 2018, **118**, 614-678.
21. J. B. Zimmerman, P. T. Anastas, H. C. Erythropel and W. Leitner, *Science*, 2020, **367**, 397-400.
22. R. A. Sheldon, *Chem. Soc. Rev.*, 2012, **41**, 1437-1451.
23. Y. Liu, N. Deak, Z. Wang, H. Yu, L. Hameleers, E. Jurak, P. J. Deuss and K. Barta, *Nat. Commun.*, 2021, **12**, 5424.
24. L. K and L. R, *Acta. Chem. Scand.*, 1972, **26**, 2005-2023.
25. K. Shimada, S. Hosoya and T. Ikeda, *J. Wood Chem. Technol.*, 1997, **17**, 57-72.
26. P. J. Deuss, M. Scott, F. Tran, N. J. Westwood, J. G. de Vries and K. Barta, *J. Am. Chem. Soc.*, 2015, **137**, 7456-7467.
27. Y. M. Questell-Santiago, M. V. Galkin, K. Barta and J. S. Luterbacher, *Nat. Rev. Chem.*, 2020, **4**, 311-330.
28. Q. Zhai, S. Han, C.Y. Hse, J. Jiang and J. Xu, *Ind. Crops. Prod.*, 2022, **177**.
29. X.-J. Shen, J.-L. Wen, Q.Q. Mei, X. Chen, D. Sun, T.-Q. Yuan and R.-C. Sun, *Green Chem.*, 2019, **21**, 275-283.
30. D. Wu, Q. Wang, O. V. Safonova, D. V. Peron, W. Zhou, Z. Yan, M. Marinova, A. Y. Khodakov and V. V. Ordomsky, *Angew. Chem. Int. Ed.* , 2021, **60**, 12513-12523.
31. M. Guo, J. Peng, Q. Yang and C. Li, *ACS Catal.*, 2018, **8**, 11174-11183.
32. Q. Fang, Z. Jiang, K. Guo, X. Liu, Z. Li, G. Li and C. Hu, *Appl. Catal. B Environ.*, 2020, **263**.
33. Y. S. Choi, R. Singh, J. Zhang, G. Balasubramanian, M. R. Sturgeon, R. Katahira, G. Chupka, G. T. Beckham and B. H. Shanks, *Green Chem.*, 2016, **18**, 1762-1773.
34. Y. G. Sun, Y. Ma, Z. Wang and J. Yao, *Bioresour. Technol.*, 2014, **158**, 307-312.
35. H. Kawamoto, *J. Wood Sci.*, 2017, **63**, 117-132.
36. M. W. Jarvis, J. W. Daily, H.-H. Carstensen, A. M. Dean, S. Sharma, D. C. Dayton, D. J. Robichaud and M. R. Nimlos, *J. Phys. Chem. A*, 2011, **115**, 428-438.
37. R. Parthasarathi, R. A. Romero, A. Redondo and S. Gnanakaran, *J. Phys. Chem. Lett.*, 2011, **2**, 2660-2666.
38. X. Yin, T. Cai, C. Liu, C. Huang, J. Wang, J. Hu, N. Li, J. Jiang and K. Wang, *Chemical Engineering Journal*, 2022, **437**.
39. K. Van Aelst, E. Van Sinay, T. Vangeel, E. Cooreman, G. Van den Bossche, T. Renders, J. Van Aelst, S. Van den Bosch and B. F. Sels, *Chem. Sci.*, 2020, **11**, 11498-11508.
40. N. Li, Y. Li, C. G. Yoo, X. Yang, X. Lin, J. Ralph and X. Pan, *Green Chem.*, 2018, **20**, 4224-4235.
41. C. Liu, L. Wei, X. Yin, X. Pan, J. Hu, N. Li, J. Xu, J. Jiang and K. Wang, *Chem. Eng. J.*, 2021, **425**.
42. X. Xiao, J. Y. Wen, Y. Y. Wang, J. Bian, M. F. Li, F. Peng and R. C. Sun, *Carbohydr. Polym.*, 2018, **195**, 303-310.
43. C. Liu, L. Wei, X. Yin, M. Wei, J. Xu, J. Jiang and K. Wang, *Ind. Crops. Prod.*, 2020, **147**.
44. A. Jaswal, P. P. Singh and T. Mondal, *Green Chem.*, 2022, **24**, 510-551.

45. A. H. Motagamwala, W. Won, C. Sener, D. M. Alonso, C. T. Maravelias and J. A. Dumesic, *Science Advances*, 2018, **4**, 9722.